Fidelity-Aware Dynamic Network Reduction of Distribution Grids with Heterogeneous IBRs

Hafiz Muhammad Faisal, Thomas Hamacher, Prashant Pant
Technical University of Munich, Germany
{hm.faisal, thomas.hamacher, prashant.pant}@tum.de

***Abstract*—Traditional network-reduction techniques struggle to accurately represent Active Distribution Networks (ADNs), especially when capturing the dynamics of inverter-based resources (IBRs) with heterogeneous control schemes. To address this gap, this work extends the German Academic Approach (GAA) to the inverter-control level, introducing a fidelity-aware workflow that couples DIgSILENT PowerFactory RMS simulations with a novel Python-based derivative-free optimization (DFO) method for automated tuning of the equivalent impedance. Validated on a CIGRÉ low-voltage benchmark, the reduced models preserve full-network dynamic behavior with high fidelity, confirmed by R^2, RMSE, nRMSE, IAE, and ISE metrics. As such, the method provides a reproducible foundation for hybrid modeling and digital-twin integration.**

***Index Terms*—Dynamic network reduction, grey-box modeling, derivative-free optimization (DFO), model fidelity.**

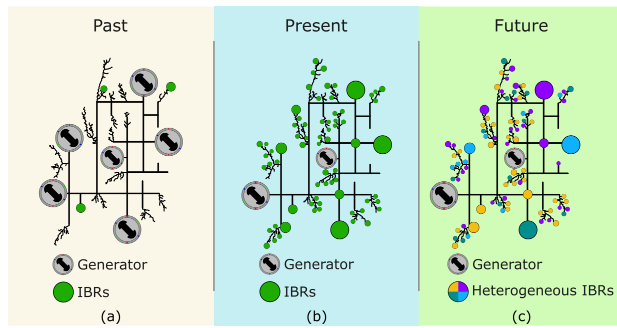

Fig. 1: Evolution of power-systems: (a) historically synchronous-machine-dominated grids, (b) present networks with mixed synchronous and grid-following inverter-based resources, and (c) future inverter-dominated systems featuring diverse grid-forming (GFM) and grid-following (GFL) controls.

I. Introduction

The Transmission System Operators (TSOs) increasingly struggle to assess dynamic stability as their grids interconnect with Active Distribution Networks (ADNs) packed with PV- and wind-based IBRs [1]. As shown in Fig. 1, this shift toward inverter-dominated operation amplifies the challenge: ADNs are difficult to model due to limited data, heterogeneous vendor-specific IBR controls, and computational constraints, making efficient Dynamic Network Reduction (DNR) essential for wide-area stability studies.

Conventional network-reduction techniques, such as Ward, REI, and coherency-based methods, were fundamentally designed to capture the electromechanical dynamics of synchronous machines and are ill-suited for converter-dominated systems governed by high-bandwidth control loops [2], [3]. While recent reduction studies have begun to address IBR-rich networks, they typically assume homogeneous control strategies or rely on detailed white-box IBR models [4]. Furthermore, the fidelity of these approaches has not yet been validated for heterogeneous networks containing both grid-forming (GFM) and grid-following (GFL) inverters, nor for practical RMS studies that represent groups of inverters using grey-box lumped equivalents.

Detailed electromagnetic-transient (EMT) modeling, while accurate, is computationally prohibitive for system-level studies [5]. RMS-domain simulation in DIgSILENT PowerFactory provides a practical alternative that efficiently represents averaged converter control dynamics. However, achieving faithful reduced models in this domain requires suitable equivalence formulations and automated parameter tuning.

Among reduction families, white-box methods rely on vendor-specific control architectures that are often unavailable [6], while black-box approaches are hindered by extensive measurement data requirements [7]. Grey-box methods offer a pragmatic compromise between interpretability and data needs. The German Academic Approach (GAA) [8] has shown strong performance in GFL-dominated grids; however, its accuracy deteriorates significantly when reducing grids with grid-forming inverters and mixed GFM–GFL controls [2].

This paper extends the GAA framework to the inverter-control level of ADNs and integrates it with an automated impedance-tuning routine using Python-based derivative-free optimization (DFO) within DIgSILENT PowerFactory [9], [10]. The resulting fidelity-aware workflow automatically adjusts the equivalent impedance (Z_{eq}) to minimize the mismatch between reduced and full-model RMS responses. Validation on the CIGRÉ LV benchmark [11] and evaluation using R^2, RMSE, nRMSE, IAE, and ISE show that the reduced models reproduce the full-network dynamics in accordance with the IEEE 2781 quantitative validation framework [12].

A. *Identified Research Gaps*

Two main research gaps motivate this work:

1) Insufficient validation of dynamic-reduction methods for ADNs with heterogeneous inverter controls.
2) The lack of a DFO-driven automation framework for parameterizing grey-box impedance models.

The work is funded by TUM SEED Center, which is a part of the DAAD program "exceed" and supported by DAAD and the German Federal Ministry for Economic Cooperation and Development (BMZ).

979-8-3315-8138-1

B. Paper Contributions

The main contributions of this paper are as follows:

1) Extension of the GAA approach from the technology level to the inverter-control level, enabling dynamic equivalence under heterogeneous inverter controls.
2) Development of a PowerFactory–Python automated workflow employing derivative-free optimization for Z_{eq} tuning within the RMS domain.

II. Methodology and Workflow

This work builds on GAA [8] to derive a reduced-order model (ROM) from the original detailed network, referred to here as the high-order system (HOS). We extend GAA to inverter-dominated ADNs by (i) introducing a control-aware aggregation that retains IBR heterogeneity across technology types (PV, wind, BESS) and control modes (grid-following vs. grid-forming, including droop and VSM variants), and (ii) closing the reduction loop with a *fidelity-aware* tuning framework. Here, *fidelity-aware* means that ROM acceptance is governed by quantitative a priori criteria, and model parameters are iteratively tuned until the ROM reproduces the HOS time-domain response at the defined study boundary.

Following an HOS reference simulation, three algorithms are executed sequentially: (i) automated identification of the internal area via breadth-first search (BFS) graph traversal and interface logging (Algorithm 1); (ii) hierarchical aggregation and pruning of internal elements using the proposed control-aware extension (Algorithm 2); and (iii) DFO-based tuning of the equivalent impedance Z_{eq} (Algorithm 3).

A. Problem Formulation

The study boundary is placed at the LV terminal of the transformer, separating the internal (reduced) and external (retained) areas. The internal impedances as seen from this boundary are represented by a single equivalent impedance

$$Z_{eq} = R + jX, \tag{1}$$

with decision vector $\theta = [R \;\; X]^{\top}$. RMS simulations of the HOS and ROM provide boundary trajectories $x(t) = \{P(t), Q(t), I(t), V(t), f(t)\}$ under identical disturbances. The impedance-tuning problem is formulated as

$$\begin{aligned} \min_{R,X} J(R,X) = \alpha \|P_{HOS} - P_{ROM}\|_2 \\ + \beta \|Q_{HOS} - Q_{ROM}\|_2, \end{aligned} \tag{2}$$

subject to parameter bounds and physical feasibility. Model acceptance is decided using the quantitative criteria in Sec. II-E; the optimisation itself focuses on aligning the active and reactive power exchange at the boundary.

B. Boundary Identification and Logging

The first algorithm automatically identifies which elements belong to the internal area to be reduced. Starting from the user-defined boundary bus, PowerFactory activates the case, reads bus and branch data, and classifies terminals through a breadth-first search (BFS). Interior DERs, loads, and feeders are logged together with transformer P/Q values, which later act as reference targets for Z_{eq} tuning.

Algorithm 1 Boundary Identification and Logging

Input: Validated CIGRÉ LV model, user-selected boundary bus b_{bd}

Graph and partitioning: Build the bus–branch connectivity graph from all in-service elements Run a breadth-first search (BFS) from b_{bd} toward the internal area Tag all reached buses and incident elements as `INTERIOR`; tag the remaining as `EXTERIOR`

Snapshot of interior DERs and loads: **foreach** *DER or load in* `INTERIOR` **do**
  record element name, technology (PV/BESS/load),
   rated power S_i, power factor, control type (Droop, VSM, GFL),
   and initial active/reactive power set-points (P_i, Q_i)

Boundary power reference: Run an AC load flow Identify the transformer whose LV terminal connects to b_{bd} Measure LV-side active and reactive power $(P_{\text{bd}}, Q_{\text{bd}})$ Store the `INTERIOR`/`EXTERIOR` partition, DER snapshot,
and boundary $(P_{\text{bd}}, Q_{\text{bd}})$ as a CSV/JSON log for Algorithm 2

return *`INTERIOR`/`EXTERIOR` sets and boundary P/Q reference*

Algorithm 2 Control-Aware Aggregation and Pruning

Input: `INTERIOR`/`EXTERIOR` sets, boundary P/Q reference

Group by control class: Partition all `INTERIOR` DERs into classes: {Droop-GFM, VSM-GFM, GFL}

foreach *control class k* **do**
  Compute total apparent-power rating

$$S_{\text{eq},k} = \sum_{i \in k} S_i$$

  Select one representative DER (e.g., DER with largest S_i) Assign aggregated steady-state values to the representative:
   active power p_{gini} proportional to $S_{\text{eq},k}$,
   reactive power q_{gini} proportional to $S_{\text{eq},k}$,
   consistent power factor $\cos\varphi_{\text{eq},k}$

Pruning: Remove all non-representative DERs belonging to each control class

Topology preservation: Retain all feeders and connections linking representatives to the boundary bus Ensure transformer interface and boundary node remain unchanged

Save the resulting reduced interior network for Algorithm 3

return *ROM with control-type representatives*

C. Control-Aware Aggregation

To extend the GAA to the inverter-control level, interior DERs are grouped by control type (GFM, GFL, droop, VSM), with the apparent power ratings summed and a single representative inverter retained per group. Non-representative elements are pruned, while feeders and boundary links are preserved to maintain connectivity and control diversity, thereby capturing heterogeneity that is neglected by conventional technology-only reductions. Fig. 2 illustrates this extended GAA, where the full internal network is aggregated into a few control-type representatives connected to the external grid via Z_{eq}.

D. Equivalent-Impedance Initialisation and DFO Tuning

The equivalent impedance is initialized from the steady-state operating point as a ”seed” for the optimization:

$$\hat{Z}_{eq} \approx \frac{V^2}{P - jQ}, \tag{3}$$

where V is the transformer LV voltage and P, Q are the measured boundary powers of the HOS. This estimate provides a physically grounded ”warm start” for (Algorithm 3). This estimate is mapped to a line type (`TypLne`) in *PowerFactory* and used as the starting point for impedance tuning.

979-8-3315-8138-1

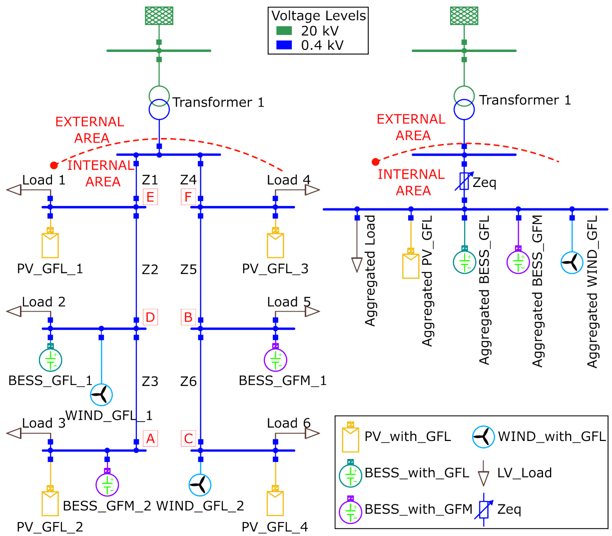

Fig. 2: Extended GAA reduction: DERs aggregated by control type, with a tunable equivalent impedance Z_{eq}.

Because each evaluation of $J(R, X)$ in (2) requires a full RMS simulation and the inverter controls yield non-smooth closed-loop responses, analytical gradients are unavailable and finite-difference estimates are unreliable. We therefore employ derivative-free optimisation (DFO), which is explicitly designed for black-box, simulation-driven objectives [9], [10].

DFO is preferred over population-based metaheuristics (e.g., GA, PSO) because the decision space is two-dimensional, and a deterministic, sample-efficient search achieves fast convergence without stochastic overhead. Algorithm 3 summarises the hybrid DFO routine, combining (i) coarse global sampling, (ii) a Hooke–Jeeves-type pattern search, and (iii) a Nelder–Mead simplex refinement, until the relative boundary P/Q errors fall below a prescribed tolerance.

E. Model-Fidelity Evaluation

Model fidelity is quantified using metrics consistent with the quantitative validation requirements of [12]: R^2, RMSE, MAE, IAE, ISE, and normalised RMSE (nRMSE). For each monitored signal, the HOS response serves as the reference trajectory, and the ROM response is evaluated under the same disturbance. A reduced model is accepted as dynamically equivalent if it satisfies:

1) $R^2 \geq 0.9$ for all monitored signals;
2) nRMSE $< 10\%$ for signals with a dynamic range of at least 5% of the mean;
3) for low-variation signals, RMSE/mean $< 2\%$ is used as a fallback criterion.

Integral indices (IAE, ISE) are used comparatively across scenarios to confirm that cumulative deviations remain small. All simulations are performed on the CIGRÉ LV benchmark [11], providing a reproducible basis for the results reported in Sec. IV.

III. System Modeling and Simulation Setup

This section specifies the benchmark network, inverter controls, disturbance definition, and RMS simulation settings

Algorithm 3 Hybrid Derivative-Free R–X Tuning

Input: P_{target}, Q_{target}, accTol, tightTol, maxEvals

Preflight: sync `pgini`, `qgini`, `sgini`, `cosgini` Activate study; get `ElmBoundary`; pick boundary link line Read latest CSV; set P_{target}, Q_{target}, transformer, tags Optional zero start: $r = 0$, $x = 0$ Seed Z_{eq} from V_{LL} and targets; set R_*, X_* Set bounds for R and X; evals $= 0$

Function `Eval`(R, X)**:**

  write per-km $r = R/d_{\text{km}}$, $x = X/d_{\text{km}}$ to `TypLne` run AC load flow; measure P_{meas}, Q_{meas} $e_P = 100 \cdot \dfrac{|P_{\text{meas}} - P_{\text{target}}|}{\max(|P_{\text{target}}|, \varepsilon_{\min})}$ $e_Q = 100 \cdot \dfrac{|Q_{\text{meas}} - Q_{\text{target}}|}{\max(|Q_{\text{target}}|, \varepsilon_{\min})}$ **if** $e_Q > e_P$ **then**

    $w_P = 1$; $w_Q = 5$

  else

    $w_P = 5$; $w_Q = 1$

  $J = (w_P \cdot e_P)^2 + (w_Q \cdot e_Q)^2$ evals $\leftarrow$ evals $+1$ **return** (J, e_P, e_Q)

Coarse sampling around (R_*, X_*) plus the seed $J_{\text{best}} = +\infty$; $R_{\text{best}} = R_*$; $X_{\text{best}} = X_*$; noValid $=$ true **foreach** *candidate* (R, X) **do**

  $(J, e_P, e_Q) \leftarrow$ `Eval`(R, X); maxErr $\leftarrow \max(e_P, e_Q)$ **if** $J < J_{best}$ **then**

    $J_{\text{best}} \leftarrow J$; $R_{\text{best}} \leftarrow R$; $X_{\text{best}} \leftarrow X$; noValid $=$ false

  if *maxErr* $\leq$ *accTol* **or** *evals* $\geq$ *maxEvals* **then**

    break

if *noValid* **then**

  $(J_{\text{best}}, -, -) \leftarrow$ `Eval`(R_*, X_*); $R_{\text{best}} \leftarrow R_*$; $X_{\text{best}} \leftarrow X_*$

Pattern search (Hooke–Jeeves): steps dR, dX about 5% with floors **while** *true* **do**

  $(J_{\text{cur}}, e_P, e_Q) \leftarrow$ `Eval`$(R_{\text{best}}, X_{\text{best}})$ maxErr $\leftarrow \max(e_P, e_Q)$ **if** *maxErr* $\leq$ *accTol* **or** *evals* $\geq$ *maxEvals* **then**

    break

  probe axes and diagonals around $(R_{\text{best}}, X_{\text{best}})$ using dR, dX **if** *any probe improves* J **then**

    update $R_{\text{best}}, X_{\text{best}}$

  else

    $dR \leftarrow dR/2$; $dX \leftarrow dX/2$

  if dR *and* dX *below floors* **then**

    break

Micro refine (simplex): small trust box (about $\pm 3\%$, min $0.02\,\Omega$); reflect/-contract within bounds **Tiny walk (coordinate):** axis steps $\approx 1\%$ (min 5 mΩ); halve on stall Stop when maxErr $\leq$ tightTol or steps are tiny **Finalise:** write $(R_{\text{final}}, X_{\text{final}})$; run load flow; report r, x, e_P, e_Q

used to evaluate the extended GAA framework. All models are implemented in *DIgSILENT PowerFactory*, with Python automation for data logging, reduction, and post-processing.

A. Benchmark Network and Boundary Definition

The framework is tested on the CIGRÉ LV benchmark [11], a typical European residential distribution network. The 20 kV/0.4 kV transformer's LV terminal is used as:

- the *boundary bus* for the extended GAA reduction, and
- *measurement point* for validation signals (V, I, f, P, Q).

Consistent with Sec. II-B, the downstream LV feeder (internal area) is reduced, while the upstream system (external area) is retained. The ROM thus replaces the detailed internal feeders with a control-aware aggregate and a single tunable impedance Z_{eq} at the boundary (Fig. 2). The network data from [11] are used to ensure traceable results.

B. Inverter Configuration and Control Scenarios

The feeder's five DERs comprise three GFL units (two PV and one wind) and two GFM BESS units (nodes A and B)

979-8-3315-8138-1

[11]. The GFL units remain unchanged. The GFM control strategy of the two BESS units defines the three scenarios:

- *Scenario A (Droop-Droop)*: Both BESS use droop.
- *Scenario B (Droop–VSM)*:Node A (Droop), Node B (VSM).
- *Scenario C (VSM-VSM)*: Both BESS use VSM control.

C. Disturbance and Simulation Setup

Dynamic equivalence is tested using a periodic load-switching disturbance at the LV terminal, toggling on/off every 1 s to generate step changes at the study boundary. The load magnitude matches the total internal steady-state active power, producing significant variations in P, Q, V, I, f without inducing faults. Simulations are performed in the RMS domain with a 10 ms time step over 7 s. This configuration provides a 700-point dataset per trajectory, which balances the need to capture IBR control dynamics (0.1–10 Hz) and multiple load-switching cycles with the requirement for a computationally lean optimization routine. Identical conditions and control settings for HOS and ROM. Boundary trajectories are exported via PowerFactory–Python and evaluated using the error thresholds Sec. II-E in Tables I–III.

IV. Results and Discussion

The proposed reduction framework is evaluated under the three GFM configurations as defined in Sec. III-B: (A) Droop–Droop, (B) Droop–VSM, and (C) VSM–VSM. For each case, the ROM produced by Algorithms 1–3 is simulated under the same disturbance as the HOS, and the transformer LV-terminal responses (P, Q, I, V, f) are compared.

A. Qualitative Comparison of Dynamic Trajectories

Fig. 3 compares HOS and ROM responses across the three scenarios (A–C) for P, Q, I, V, f at the boundary bus. Overall, the ROM closely tracks the HOS in both transient and steady-state behavior. Minor steady-state offsets in P and Q arise from the simplification of distributed line losses and shunt capacitances into a single lumped impedance ($R_{eq} + jX_{eq}$), alongside the use of aggregated controller setpoints. Nevertheless, all signals remain well under the thresholds.

B. Quantitative Fidelity Assessment

To address numerically ill-conditioned nRMSE values from signals with small dynamic ranges ($< 5\%$ of the mean), the ROM is evaluated using the IEEE 2781 criteria [12]:

$$\text{nRMSE} < 10\% \quad \text{or} \quad \frac{\text{RMSE}}{\text{mean}} < 2\%.$$

For transparency, full error tables for scenarios A–C (Tables I–III) and a compact summary (Table IV) are provided.

C. Discussion

From the simulation results, three major insights emerge:

1) Robustness to control heterogeneity: High accuracy across droop (A), mixed (B), and VSM (C) scenarios confirms the applicability of the extended GAA beyond classical droop networks.
2) Reproduction of virtual inertia effects: The ROM preserves the expected slower VSM settling and enhanced frequency damping in Scenarios B and C, despite reducing network to a single Z_{eq} and representative units.
3) Boundary dynamic equivalence preserved: All boundary dynamics (power, current, voltage, frequency) remain within the IEEE 2781 criteria [12].

TABLE I: Scenario A: Droop–Droop Fidelity Metrics

Signal	R^2	nRMSE (%)	RMSE/mean (%)	Valid?
P	0.9996	77.87*	1.35	Yes
Q	0.9983	0.87	–	Yes
I	0.9994	88.88*	1.31	Yes
V	0.99999	1.25	–	Yes
f	0.9832	1.84	–	Yes

**nRMSE invalid (dynamic range $< 5\%$ of mean); RMSE/mean used instead.*

TABLE II: Scenario B: Droop–VSM Fidelity Metrics

Signal	R^2	nRMSE (%)	RMSE/mean (%)	Valid?
P	0.9975	39.34*	0.71	Yes
Q	0.9991	67.44	–	No†
I	0.9971	32.82*	0.50	Yes
V	0.99998	4.21	–	Yes
f	0.9798	1.23	–	Yes

**nRMSE invalid (dynamic range $< 5\%$ of mean); RMSE/mean used instead.*
†Valid nRMSE $> 10\%$ due to droop–VSM transient interaction. [4].

TABLE III: Scenario C: VSM–VSM Fidelity Metrics

Signal	R^2	nRMSE (%)	RMSE/mean (%)	Valid?
P	0.9969	70.08*	1.35	Yes
Q	0.9988	1.67	–	Yes
I	0.9954	80.86*	1.31	Yes
V	0.99999	1.25	–	Yes
f	0.9906	0.74	–	Yes

**nRMSE invalid due to low dynamic range; RMSE/mean used instead.*

TABLE IV: Compact Summary of Fidelity Across All Scenarios

Metric	A	B	C
Min R^2	0.983	0.980	0.991
Max accepted error (%)	1.84	4.21	1.67
Signals requiring RMSE/mean	P, I	P, I	P, I
Max RMSE/mean (%)	1.35	0.71	1.35

Scenario C's shorter transients stem from the tighter VSM active power-frequency droop ($m_p = 1\%$) versus the Droop-controlled units ($m_p = 5\%$), providing a stiffer response and faster recovery. Overall, the results confirm that the proposed fidelity-aware reduction maintains dynamic accuracy across diverse inverter-dominated scenarios while substantially simplifying the internal ADN model.

V. Conclusion

This work presented a grey-box extension of the GAA approach for RMS-domain model reduction of inverter-dominated ADNs, using a PowerFactory–Python loop with DFO-based Z_{eq} tuning. Validation on the CIGRÉ LV benchmark shows high fidelity for P, V, I, and f responses (typical $R^2 \geq 0.98$, RMSE/mean $\leq 1.5\%$) across all scenarios except droop–VSM, where reactive power deviation reflects the expected transient interaction between dissimilar GFM

979-8-3315-8138-1

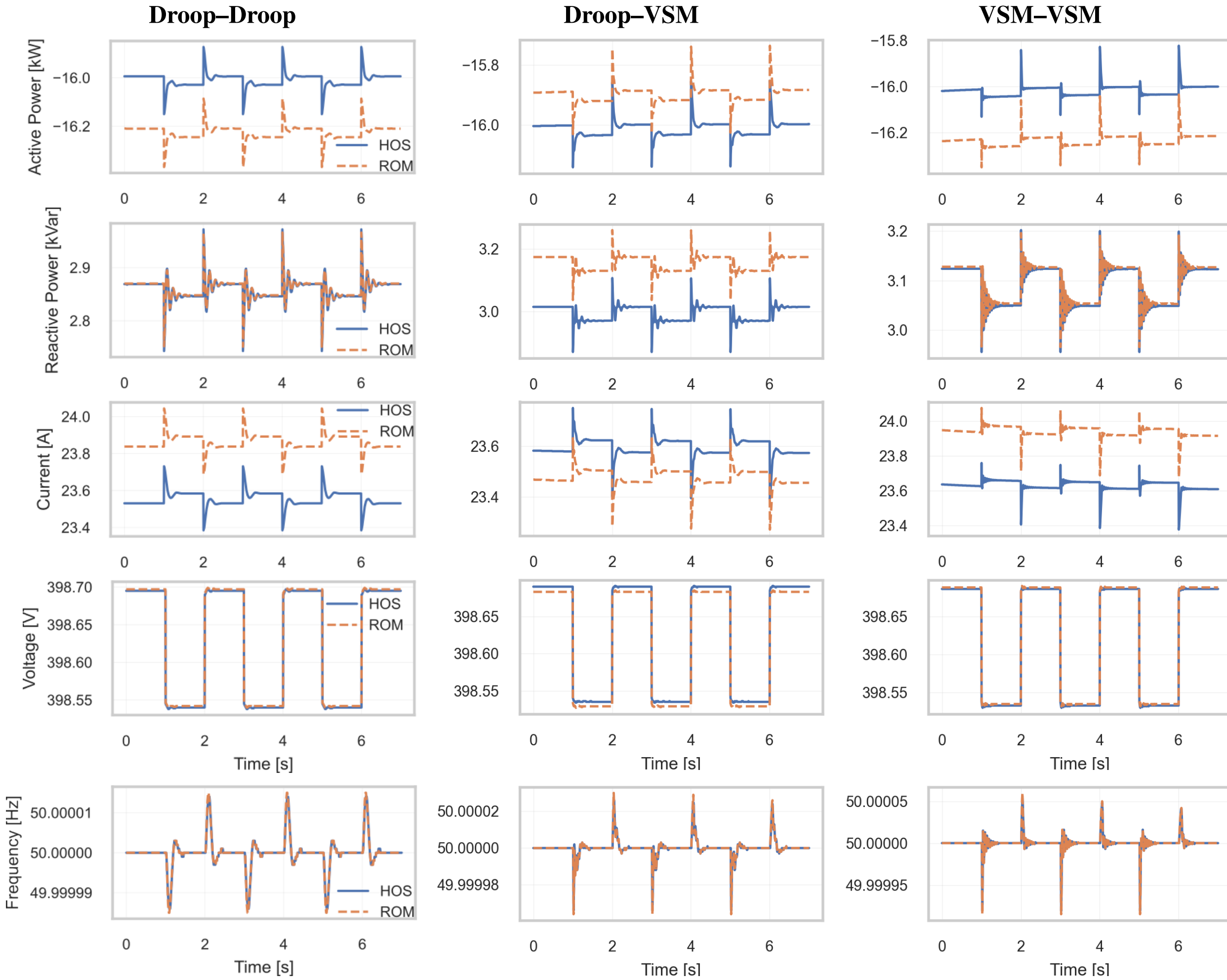

Fig. 3: Comparison of HOS (solid) and ROM (dashed) at the boundary bus across three IBR configurations and five monitored signals.

regulators [4] rather than a limitation of the workflow. The method eliminates manual impedance calibration, yields reproducible ROMs, and offers a practical trade-off between fidelity, interpretability, and computational efficiency for controller validation and large-scale grid studies.

Future work will focus on: (i) extending validation to unbalanced faults and short-circuit events; (ii) augmenting the DFO objective to include voltage and frequency, and (iii) developing hybrid grey/black-box models that combine equivalent grid models with data-driven inverter/prosumer surrogates.

References

[1] F. Conte, F. D'Agostino, and F. Silvestro, "10 - equivalent dynamic modeling of active distribution networks for tso-dso interactions," in *Decentralized Frameworks for Future Power Systems*, M. P. Moghaddam, R. Zamani, H. H. Alhelou, and P. Siano, Eds. Academic Press, 2022, pp. 227–275. [Online]. Available: https://www.sciencedirect.com/science/article/pii/B9780323916981000029

[2] J. Ungerland and P. Pant, "Challenges of modelling equivalent active distribution grids under consideration of grid forming inverters," in *Conference Proceedings of the 19th Wind Integration Workshop*. Piscataway: IEEE, 2020.

[3] O. Ajala, N. Baeckeland, B. Johnson, S. Dhople, and A. Domínguez-García, "Model reduction and dynamic aggregation of grid-forming inverter networks," *IEEE Transactions on Power Systems*, vol. 38, no. 6, pp. 5475–5490, 2023.

[4] L. Wang, Z. Liu, J. Ma, and X. Zhang, "Model reduction and dynamic aggregation of grid-forming inverter networks," *IEEE Transactions on Power Systems*, vol. 38, no. 6, pp. 5140–5153, 2023.

[5] S. Subedi, M. Rauniyar, S. Ishaq, T. Hansen, R. Tonkoski, M. Shirazi, R. Wies, and P. Cicilio, "Review of methods to accelerate electromagnetic transient simulation of power systems," *IEEE Access*, vol. 9, pp. 89 714–89 731, 2021, publisher Copyright: © 2013 IEEE.

[6] Electric Power Research Institute (EPRI), "Concepts of model quality testing for inverter based resources," EPRI, Palo Alto, CA, Tech. Rep. 3002027506, 2023.

[7] N. Guruwacharya, S. Chakraborty, G. Saraswat *et al.*, "Data-driven modeling of grid-forming inverter dynamics using power hardware-in-the-loop experimentation," *IEEE Access*, vol. 12, 2024.

[8] J. C. Boemer, "On stability of sustainable power systems: Network fault response of transmission systems with very high penetration of distributed generation," Ph.D. dissertation, Delft University of Technology, Delft, The Netherlands, June 2016. [Online]. Available: https://doi.org/10.4233/uuid:78bffb19-01ed-48f9-baf6-ffb395be68a0

[9] A. R. Conn, K. Scheinberg, and L. N. Vicente, *Introduction to Derivative-Free Optimization*. Philadelphia, PA: SIAM, 2009.

[10] J. Larson, M. Menickelly, and S. M. Wild, "Derivative-free optimization methods," *Acta Numerica*, vol. 28, pp. 287–404, 2019.

[11] CIGRÉ Task Force C6.04.02, *Benchmark Systems for Network Integration of Renewable and Distributed Energy Resources*. Paris, France: CIGRÉ, 2014.

[12] *IEEE Guide for Load Modeling and Simulations for Power Systems*, IEEE Power and Energy Society Std. IEEE Std 2781-2022, 2022.

979-8-3315-8138-1